EurJIC
European Journal of Inorganic Chemistry

Chemistry Europe
European Chemical Societies Publishing

Accepted Article

Title: Electronic and Steric Manipulation of the Agostic Interaction in benzo[h]quinolone Complexes of Pd(II) and Implications for the Formation of η1-Pd–C Bonds

Authors: Alastair James Nielson, John Harrison, Arif Sajjad, and Peter Schwerdtfeger

To be cited as: *Eur. J. Inorg. Chem.* 10.1002/ejic.202000348

Link to VoR: https://doi.org/10.1002/ejic.202000348

WILEY-VCH

10.1002/ejic.202000348

WILEY-VCH

FULL PAPER

Electronic and Steric Manipulation of the Agostic Interaction in benzo[*h*]quinoline Complexes of Pd(II) and Implications for the Formation of η¹-Pd–C Bonds

Alastair J. Nielson,*[a] John A. Harrison,*[a] M. Arif Sajjad[a] and Peter Schwerdtfeger[b]

Abstract: Structures and properties were obtained by density functional (DFT) calculations for the complexes [$PdCl_2$(L)] (L = benzo[*h*]quinolines) containing aromatic ring agostic interactions. The inflexibility of the benzenoid rings of the ligands keep the structures of the complex relatively constant when electron withdrawing substituents are added to the aromatic ring *para* to the agostic carbon but electron donation causes a change to η¹-Pd–C bond complexes in which agostic donation is significantly reduced and π-syndetic donation no longer features. Increasing the steric size at the α-carbon through the series H, Me, $CHMe_2$, CMe_3 or Ph, changes the manner in which the ligand sits in relation to the coordination plane but a change in the way the nitrogen atom of the ligand tilts in relation to the coordination plane does not effectively reduce the agostic or syndetic donations. CPh_3 reduces the agostic donation but not the syndetic donation and C(Ph-2,6-Me_2) turns both donations off and installs η² π-donation on one aromatic ring. Placing *ortho*-substituents on the ring can influence the interplay of electronic and steric effects when η¹-Pd complexes are formed.

Introduction

Cyclometallation reactions,[1] important in the development of transition metal catalysed C–H bond functionalisations,[2] have been shown to rely on the agostic interaction[3] to activate the C–H bond. In this regard, we have recently reported that in addition to the known participation of aromatic ring agostic C–H bond electron density donation to palladium occurring during the accepted Concerted Metallation Deprotonation/Ambiphilic Metal Ligand Activation (CMD/AMLA) mechanism for cyclopalladation,[4] there can be additional donation to the metal centre which involves π or σ-bond orbital electron density from the ring localized uniquely in the vicinity of the carbon atom to be metallated.[5] This type of donation which appears to assist the agostic interaction, was termed 'syndetic donation' and pointed to a much more complex interaction overall.[5a,b] We have also referred to the involvement of electrostatic attraction and repulsion being important based on the charge differences[5] and the nature of this charge separation has been expanded in a recent in-depth investigation of this coulombic component by other workers which showed a multi-pole environment for the agostic interaction.[6]

A key feature of our computational studies involving aromatic ring agostic interactions has been to assess the effect of adding electron withdrawing or donating substituents to the aromatic ring to try and influence the various contributing components.[5] In addition, we have also looked at how steric aspects carry out this function.[5c,d] These studies have focused on aromatic ring systems where the ring can rotate to assist the interaction or distort outside the agostic C–H bond ring system to achieve the same result. We have now turned to a much less flexible system in an attempt to force a very close agostic C–H bond approach to ascertain how the various components can be influenced. We present here the results of computation studies on the electronic and steric manipulation of the agostic bonding characteristics in such a ligand, with a focus on implications of structural changes in the molecules.

Results and Discussion

1) DFT structure and properties of [$PdCl_2$(benzo[*h*]quinoline)]. As an entry into the characteristics of close approaches made to palladium, the benzo[*h*]quinoline ligand (figure 1) was chosen on the basis that with two benzenoid ring junctions present, the system would be expected to be mostly inflexible which should allow little opportunity for the C–H hydrogen to avoid close contact with the metal centre in an

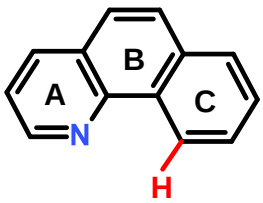

Figure 1. Structure of the benzo[*h*]quinoline ligand showing the A, B and C rings and the potential C–H bond agostic hydrogen.

[a] *Prof. Dr. A. J. Nielson, Dr. J. A. Harrison, Dr. M. A. Sajjad*
Institute of Natural and Mathematical Sciences, Massey University Auckland, Private bag 102904, North Shore Mail centre, Auckland, New Zealand
E-mail: a.j.nielson@massey.ac.nz
[b] *Prof. Dr. P. Schwerdtfeger*
Centre for Theoretical Chemistry and Physics, Institute of Advanced Studies, Massey University Auckland, Private bag 102904, North Shore Mail centre, Auckland, New Zealand.
E-mail: peter.schwerdtfeger@gmail.com

Supporting information for this article is given via a link at the end of the document.

agostic interaction once the N atom coordinates. In addition, the ligand is relevant to the present study of palladium-based agostic interactions as it is known to cyclometallate for this metal.[7] In a previous study where we looked at the anagostic separations in rhodium complexes containing the benzo[*h*]quinoline ligand (L in [RhCl(CO)$_2$(L)]), it was found that electrostatic repulsion keeps the C–H bond hydrogen away from the Rh centre and electrostatically attractive Rh···C interactions are prevented from closing up by ligand inflexibility.[8]

For the present computational study, we have used the PBE-D3 functional[9] that includes dispersion which has been shown to be a fundamental component of agostic interactions,[10] is known to perform well for this type of weak interaction[11] including the coulombic component[6] and is the functional we have used in our other computational work on agostic interactions.[5] In terms of the type of complex we have used, agostic structures for [PdCl$_2$(benzo[*h*]quinoline)] complexes were calculated which contain chloro ligands so that the agostic hydrogen would not be influenced by ligand proximity as is found in the CMD/AMLA mechanism involving acetato ligands.[4,5d]

The energy minimised agostic structure for [PdCl$_2$(benzo[*h*]quinoline)] (**1**) (figure 2) shows that the ligand rotates into but slightly above the N and Cl atom coordination plane so that the C^2-hydrogen (numbering used for the pertinent sections of the aromatic C-ring containing the agostic interaction are shown in figure 2a) lies slightly below the coordination plane and the C^2-carbon slightly above it so that the Pd···H separation is 1.768 Å and the Pd···C^2 separation is 2.219 Å (figures 2a and 2b, all relevant metrics in table 1). As seen in figure 2b, the A-ring section of the ligand lies quite flat with respect to the coordination plane and the extent of this is shown by the Cl–Pd–N–C torsion angle involving the Cl ligand that lies *cis* to N, being large at 156.1°. The angle the C-ring makes with the coordination plane at 146.4° (Ar/CP torsion in table 1) Is not much smaller which reflects the structural inflexibility of the ligand. In other complexes

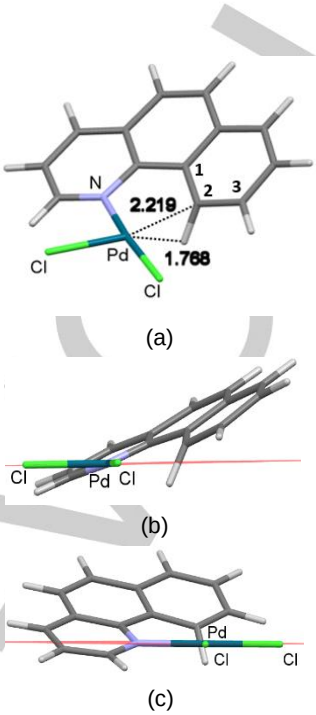

Figure 2. Computed structure for the agostic [PdCl$_2$(benzo[*h*]quinoline)] complex (**1**). (a) Capped stick model for the energy minimised structure showing the coordination geometry, ring numbering and close approaches (Å). (b) View down the trans-Cl–Pd–N bond. The orange line traces a line parallel to the coordination plane. (c) View down the Cl–Pd bond *trans*-to the agostic C–H bond.

Table 1. Selected Structural Data for Complexes **1** - **5**

Complex	**1**	**2**	**3**	**4**	**5**
Para-Substituent	**H**	**SO$_2$Cl**	**N$_2$PO(OEt)$_2$**	**B(OH)$_3^-$**	**S$^-$**
Bond Length					
Pd-N	2.061	2.060	2.059	2.057	2.054
Pd-Cl(*trans*)	2.274	2.269	2.273	2.315	2.357
Pd-Cl(*cis*)	2.277	2.273	2.277	2.295	2.303
C-H	1.166	1.173	1.169	1.151	1.127
Separations					
Pd···H	1.768	1.756	1.766	1.826	1.989
Pd···C^1	2.934	2.936	2.938	2.939	2.921
Pd···C^2	2.219	2.199	2.193	2.204	2.162
Pd···C^3	3.290	3.255	3.246	3.280	3.239
Torsions					
Ar/CP	146.4	144.8	145.7	149.8	151.4
Pd-N-C-C^1	5.9	5.1	5.2	5.0	6.4
N-C-C(1)-C^2	8.6	8.6	8.0	9.2	10.6
Cl-Pd-N-C	156.1	154.7	155.4	161.0	164.0
C-H bond deformation	30.4	31.4	32.6	33.1	39.1
Angles					
Pd-N-C$_p$ deformation[a]	8.7	8.1	8.1	8.2	9.2
Pd-N-C	113.9	114.1	114.0	114.1	114.1
N-C-C^1	117.3	117.2	117.3	117.3	116.5
Pd···H-C	96.2	95.2	94.5	92.7	82.9
Pd···C-H	52.4	52.7	53.4	55.8	65.9

[a] C*p* = A-ring *para*-carbon; measured angle is Pd-N-C*p*; deformation angle shown is 180°– Pd-N-C*p* angle.

we have calculated structures for where the analogous C-ring can rotate or there are distortions outside the aromatic ring containing the agostic C–H bond, these angles are much steeper[5] (*ca* 129°) which presents more of the C-ring plane to the metal centre.

The positioning of the aromatic C-ring with respect to the coordination plane, now places the C^2–H bond facing the palladium centre so that a line drawn through the coordination plane and projected to the right, cuts this bond half way down (figure 2b) and a line-of-sight through the Cl–Pd bond points slightly to the right of it (figure 2c). The N–C–C^1–C^2 torsion angle of only 8.6° shows again that the benzo[*h*]quinoline ligand hardly distorts from planarity and reflects the ligand inflexibility.

As to how the ligand manages to cooordinate at all with an agostic interaction involved is achieved partly by the C^2–H bond distorting significantly out of the plane of the aromatic C-ring (C–H deformation angle in table 1, 30.4°). This type of distortion is well recorded for the somewhat rare aromatic ring agostic C–H bond interactions[3b,12] but is much larger in magnitude in the present case than found for the computed stuctures of less constrained aromatic ring systems (ca. 20°)[5]. The other way coordination is achieved at all is seen at the benzo[*h*]quinoline ligand nitrogen atom where the pyridine A-ring is not in the same plane as the *trans*-related Pd–Cl bond but deviates by 8.7° (the Pd–N–C_p deformation angle of 8.7° in table 1 is actually measured as 171.3°; C_p is the carbon at the *para*-position of the nitrogen A-ring).

To gain insight about the orbital interactions involved in the close approaches of the agostic C–H bond in **1**, we have used Natural Bond Orbital (NBO) analysis[13] which provides an estimation of the energies involved using the second order perturbation energy, *E*(2). It should be noted here that this type of analysis is required as orbital interactions obtained from molecular orbitals are descriptive only and do not give a meaningful quantified approach[13]. Whereas the *E*(2)values are not comparable to other types of energies, they are themselves directly comparable and we have used them previously in this manner for series comparisons within the same functional and basis set for both agostic and anagostic interactions.[5,8] At this point it should be emphasised that an agostic interaction is not an example of a hydrogen bond due to both the H atom and Pd centres possessing positive charges. In this regard, the applicability of NBO analysis to hydrogen bonded dimers has been the subject of some discussion due to basis set superposition error (BSSE)[14] but recent work has shown that BSSE doesnot overtly effect agostic interactions.[6,15]

The NBO analysis for the agostic C^2–H bond for **1** (table 2), shows C−Hσ bond electron density donations to both the Pd−Clσ^*(*trans*) and Pd−Clσ^*(*cis*) orbitals with *E*(2) values of 52.0 and 3.6 kcal mol^{-1} respectively. The dual nature of the donations is similar to other $PdCl_2$(ligand) agostic complexes we have reported but the total *E*(2) value for **1** of 55.6 kcal mol^{-1} is slightly lower than that observed for these others [range of *E*(2) values, 61.7 to 73.7 kcal mol^{-1}][5a-d] but higher than in a variety of C–H bond activation ligand-directing groups when the coordinating atom is oxygen rather than nitrogen [range of *E*(2) values, *ca* 30 to 40 kcal mol^{-1}].[5e]

Looking at the syndetic π-donations (table 2) which are from the C^2−C^3 aromatic ring π-orbital to the same metal based orbitals as are the agostic donations, the *E*(2) value of 12.8 kcal mol^{-1} for the two is much lower than that seen for other $PdCl_2$(ligand) agostic complexes where the *E*(2) values range from 61.7 to 73.7 kcal mol^{-1}.[5a,b] This significant change for **1**, appears to be related in part to the N–C–C^1–C^2 torsion angle of 8.6° which as already mentioned shows that the benzo[*h*]quinoline ligand hardly distorts from planarity and does not allow the aromatic C-ring to face the palladium centre as in the other more flexible $PdCl_2$(ligand) agostic complexes where the aromatic ring can rotate or distort away from the metal

Table 2. NBO Analysis *E*(2) data for Complexes **1** – **5**.

Complex	**1**	**2**	**3**	**4**	**5**
Para-Substituent	**H**	**SO_2Cl**	**$N_2PO(OEt)_2$**	**$B(OH)_3^-$**	**S^-**
LP N to Pd	90.5	89.9	90.7	70.8	70.8
LP N to Pd	9.6	9.3	9.4	5.6	3.9
Total	100.1	99.2	100.1	76.4	71.7
Agostic					
C−Hσ -Pd−Clσ^*(*trans*)	52.0	55.3	54.0	14.5	11.0
C−Hσ - Pd−Clσ^*(*cis*)	3.6	3.8	3.6	-	-
Total agostic	55.6	59.1	57.6	14.5	11.0
Syndetic					
C^2−$C^3\pi$ - Pd−Clσ^*(*trans*)	11.1	11.0	12.2	-	-
C^2−$C^3\pi$ -Pd−Clσ^*(*cis*)	1.7	1.7	1.9	-	-
Total π-syndetic	12.8	12.7	14.2	-	-
C^1−$C^2\sigma$ - Pd−Clσ^*(*trans*)	1.8	1.9	1.9	1.8	2.2
C^1−$C^2\sigma$ -Pd−Clσ^*(*cis*)	0.4	0.5	0.5	-	-
Total σ-syndetic	2.2	2.4	2.4	1.8	2.2
C^2−$C^3\sigma$ - Pd−Clσ^*(*trans*)	0.3	0.4	0.3	-	-
C^2−$C^3\sigma$ -Pd−Clσ^*(*cis*)	-	-	-	-	-
Total σ-syndetic	0.3	0.4	0.3	-	-
Back Donation					
Pd - C−Hσ^*	9.7	10.3	9.9	5.7	3.1
Pd - C^2−$C^3\pi$	3.7	3.3	3.5	-	-
Pd - C^2−$C^3\sigma$	0.8	0.9	0.9	0.9	1.0
Pd - C^1−$C^2\sigma$	0.6	0.7	0.7	0.6	0.7

centre (comparative N–C–C^1–C^2 torsion angles range from 14.7 to 18.5°)[5]. There are some other small positioning changes which collectively also contribute to the difference but the benzo[*h*]quinoline ring inflexibility appears to be the most important factor. In general, the C^1–C^2 syndetic σ-donation for **1** at 2.2 kcal mol^{-1} is marginally larger than the other complexes mentioned. In NBO terms, small *E*(2) values such as these are at the limit of the analysis[16] but they are quoted here for comparative indications only.

2) Electronic Effects

In our previous computational work on agostic interactions with the more flexible acetophenone and 1-tetralone oxime ligands, we found that there was a pronounced substituent electronic effect on the strength of both the agostic and π-syndetic donations and that both components could be manipulated by changing the electronic environment.[5a-d] In these studies and the present one, we have used substituents on the carbon that lies *para*-to the agostic C^2-carbon as in general aromatic ring substituent chemistry, the effects are more pronounced at this position[17] compared to *meta*-substituents[17] and the *ortho*-position can involve both steric and electronic effects.[18]

For the present study, as with our previous computational work, we have used the strongest electron donating or withdrawing groups available to influence either the σ or π systems of the aromatic ring but not both at the same time. The substituent used for σ-electron withdrawing is SO_2Cl (*F* value 1.16; *R* value –0.05[17]), complex (**2**), π-electron withdrawing, $N_2PO(OEt)_2$ (*F* value -0.05; *R* value 0.79[17]), complex (**3**); σ-electron donation $B(OH)_3^-$ (*F* value -0.42; *R* value -0.02[17]), complex (**4**) and π-electron donation, S^- (*F* value -0.03; *R* value -1.24[17]), complex (**5**) (see scheme 1). The effects were then compared to where the substituent is H, similar to Hammett protocol.[18] It should be remembered here that as the substituents do not have the same electron donating or withdrawal abilities in terms of *F* or *R* values,[17] direct comparison of data magnitudes are unrealistic. However, trends relating to electron withdrawal or donation can be made and these are used throughout the present electronic influence studies.

Based on the C^2–H bond length which can be used as a measure of the agostic donation as electron donation to the metal weakens and thus lengthens it, σ-electron withdrawing group SO_2Cl in complex **2** increases the agostic donation marginally compared to **1** (C^2–H bond lengths, 1.173 and 1.166 Å for **2** and **1** respectively, see comparison of the metrics in table 1) and this occurs when the only significant change to the structural features is a small decrease in the Pd···C^2 and Pd···C^3 separations (distances 2.199 and 2.219 Å; 3.255 and 3.290 Å) meaning that the C^2 and C^3 ring carbons have moved closer to the metal.The small increase in agostic donation is confirmed by NBO data where the *E*(2) values are 59.1 and 55.6 kcal mol^{-1} for **2** and **1** respectively. This seemingly unusual increase in agostic donation with strong σ-withdrawal from the aromatic ring was also found for the SO_2Cl substituent in the less flexible nitrogen ligands we have studied earlier and was related to the C-H bond electron density becoming more symmetrical so that increased electron density was available for agostic donation.[5b] However, we have not looked at this effect for the present benzo[*h*]quinoline ligand. For the other donations, inspection of

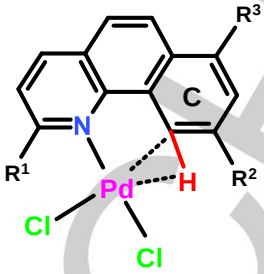

(**1**) R^1, R^2, R^3 = H
(**2**) R^1, R^2 = H, R^3 = SO_2Cl
(**3**) R^1, R^2 = H, R^3 = $N_2PO(OEt)_2$
(**4**) R^1, R^2 = H, R^3 = $B(OH)_3^-$
(**5**) R^1, R^2 = H, R^3 = S^-

Scheme 1. Structures showing the electronic substituents on ring C.

table 2 shows that the syndetic π and σ-donations to the metal as well as the Pd to C–H* orbital back-donation do not vary much individually.

In our previous work on agostic interactions where we have utilised more flexible nitrogen ligands, we noted that an increase in negative charge at the agostic carbon occurs along with shortened Pd···C separations[5a-d] and as mentioned in the introduction, a more indepth study has indicated the importance of colombic effects in agostic interactions in general.[6] In this regard it is noted that the small decrease in the Pd···C^2 separation in going from **1** to **2** (2.219 to 2.199 Å) involves a small decrease in negative charge on C^2 (see table S4 in the ESI) [*q*(H) values (QTAIM atomic basin charge[19]), -0.0809 and -0.0717 *e*] which is associated with a slight increase in positive charge on Pd [*q*(H) values, 0.6207 and 0.6312 *e*).

Turning to the $N_2PO(OEt)_2$ substituent which is somewhat uncommon but does have the strongest π-withdrawing effect (*R* value 0.79[17]), the C^2–H bond length for complex **3**, is only a little shorter than for the SO_2Cl substituent in **2** (1.169 and1.173 Å respectively) indicating that it has very little effect on the agostic interaction. The Pd···C^2 separation is a little shorter at 2.193 Å compared to 2.199 Å but as with the other metrics, there is very little change. The NBO analysis shows little change for the agostic and syndetic donations as is found for the Pd to C–H* orbital back-donation and there is little change in the various atomic charges. Overall, σ and π-withdrawing substituents have very little effect on the various donations and charges. This contrasts with the more flexible nitrogen ligands where the effects are more discernable.[5]

For σ-donating substituent $B(OH)_3^-$, table 1 shows that the metrics change in that the C^2–H bond length for complex **4** is now significantly shorter than for where the substituent is H in complex **1**(1.151 and 1.166 Å respectively) indicating that the agostic interaction has been reduced in magnitude. This occurs

when the Pd···C^2 separation at 2.204 Å in **4** has dereased from that found for **1** (2.219 Å) and the Pd···H separation has increased a little (1.826 Å compared to 1.768 Å). Also, the Ar/Cp torsion has flattened a little (149.8 and 146.4° in **4** and **1** respectively) as has the Cl–Pd–N–C torsion (161.0 versus 156.1°) whereas the other metrics are not significantly affected. The NBO data now shows there is a signifiant impact with $B(OH)_3^-$ as the substituent, in that the total lone pair donation from nitrogen to the metal is reduced [*E*(2) values, 76.4 and 100.1 kcal mol^{-1} for **4** and **1** respectively], the total agostic donation is much smaller [*E*(2) values, 14.5 and 55.6 kcal mol^{-1}] and the π-syndetic donation has been completely switched off. There still remains a small amount of σ-syndetic donation that was present in **1** but with the much reduced agostic donation, the Pd to C–H* backdonation is significantly reduced [*E*(2) values, 5.7 and 9.7 kcal mol^{-1} for **4** and **1** respectively].

Further inspection of the NBO data shows that there are components present consistent with the presence of a Pd–C σ-bond (see table S5 of the ESI) so that the complex is now an η^1-complex of palladium[20] but essentially on the fairly weak side as the Pd–C bond distance of 2.204 Å is to the upper end of of the values for this type of bond for palladium.[20] For the more flexible ligands we have reported previously, the $B(OH)_3^-$ substituent did not achieve η^1-complex formation.[5] Inspection of the atomic charges in table S4 of the ESI shows that the C^2-atomic charge at -0.1133 *e* for this type of complex is now much more negative than in **1** (-0.0809 *e*) which reflects the build-up of electron density at C^2 resulting from the *para*-substituent donation. The H-atomic charge has become slightly less positive (0.0507 *e* in **4**; 0.0566 *e* in **1**) and the metal less positive with the formation of the η^1-Pd–C bonding system (0.6004 *e* in **4**; 0.6207 *e* in **1**).

Placing the strongly π-donating S^- substituent in the *para*-position in complex **5**, now causes the C–H bond length to drop to 1.127 Å indicating even less agostic donation than in $B(OH)_3^-$ complex **4** and the Pd···C^2 separation closes right down to 1.162 Å which is now well inside the range of values recorded for η^1-palladium complexes.[20] It is now seen that the C^2–H bond deformation has moved out to the value of 39.1° which is significantly larger in magnitude than for complexes **1**-**4** where the range is 30.4 to 33.1°. The other metrics are however not significantly different to $B(OH)_3^-$ complex **4**.

Inspection of the NBO data for **5** shows that the *E*(2) value for the agostic donation has reduced to 11.0 kcal mol^{-1} compared to 14.5 and 55.6 kcal mol^{-1} in **4** and **1** respectively. As found for **4**, there is no π-syndetic donation observed for **5**, the σ-syndetic donation is similar and along with the reduced agostic donation already mentioned, the Pd to C–H* backdonation is slightly less [*E*(2) values 3.1 and 5.7 kcal mol^{-1} for **5** and **4** respectively]. The C^2-atomic charge in **5** is slightly less negatve in comparison to **4** (-0.1077 and -0.1130 *e*) whereas with the S^- substituent present, the Pd atomic charge is significantly less positive (0.5684 *e* in **5**; 0.6004 *e* in **4**). The NBO analysis also shows the η^1-Pd–C^2 bonding as in **4** but now there is significant charge density donated from S^- through the aromatic ring π-orbitals to the Pd–C^2 bonding orbitals (see table S5 in the ESI). In this case, the C^1–C^2 and C^2–C^3 ring bond distances are only a little longer than the other ring C–C bond distances indicating that the C^2-carbon does not attain much sp^3 character. In the more flexible ligands with the S^- substituent we have studied, some sp^3 character has been observed[5] but it is not found to any extent in the present less-flexible benzo[*h*]quinoline ligand.

2) Steric effects at the Carbon *ortho* to nitrogen in Ring A

In the present complexes, the benzo[*h*]quinoline ligand coordinates at a fairly flat angle as shown in complex **1** where the Ar/Cp torsion angle is 146.4° and the Cl–Pd–N–C torsion angle is 156.1°. As such, the C–H bond hydrogen lying *ortho* to the aromatic A-ring nitrogen atom lies slightly below the coodination plane (see figure 2) and quite close to the adjacent chloro ligand with a Cl···H distance of 2.590 Å. With this relatively close approach and the Cl atomic charge of –0.4634 *e* and H atomic charge of 0.0874 *e*, a weak hydrogen bond can be expected but probably is not strong enough to influence the coordination mode of the ligand. Inspection of the NBO data shows that the backbonding from Cl lone pairs to the C–H* orbital has a total *E*(2) value of 2.3 kcal mol^{-1} which is weak for this component of a hydrogen bond.

Given the closeness of the *ortho*-hydrogen in the nitrogen ring A to this Cl ligand, it was of interest to see if an increase in substituent size at this position could exert a steric effect and disrupt the agostic interaction at the other side of the molecule. In our previous work with the more flexible ligands it was found that a steric clash at this part of the molecule could affect both the agostic and syndetic components[5] and so in the present work the interest was to ascertain if these components could be detuned or manipulated even to the point of completely switching them off.

The substituent size was initially the progression shown in scheme 2 from methyl through to *tert*-butyl (complexes **6** – **8**) and Ph (complex **9**). Looking at the change in C^2–H bond

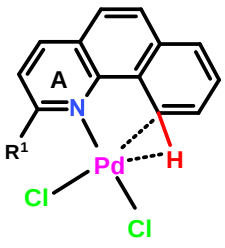

(**6**) R^1 = Me
(**7**) R^1 = $CHMe_2$
(**8**) R^1 = CMe_3
(**9**) R^1 = Ph
(**10**) R^1 = CPh_3
(**11**) R^1 = $C(Ph\text{-}2,6\text{-}Me_2)_3$

Scheme 2. Structures showing position of the steric substituents on ring A of the benzo[*h*]quinoline ligand.

length as an indicator of the agostic interaction (the metrics for all the complexes are contained in table S2 of the ESI whereas graphical representations accompanied by data are used here for some metrics for ease of visualisation of the changes), methyl and isopropyl groups do not change significantly from the value of 1.166 Å and even with a *tert*-butyl group the value only drops to 1.156 Å but reaches 1.164 Å for a phenyl (Ph) group (see the graphical trend in figure 3).

In terms of the other metrics for these substituents, the Ar/Cp torsion angles reduce in magnitude as do the Cl–Pd–N–C torsion angles (see figure 4) which reach 121.7° for CMe_3 (156.1° for R = H) indicating that the aromatic ring containing the agostic interaction is able to face the coordination plane at steeper angles. Progressing through the substituent series, the

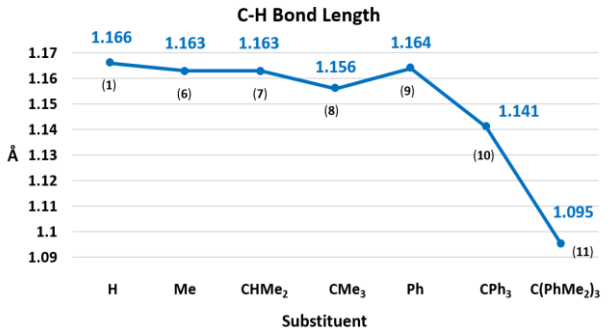

Figure 3. Graphical presentation of the change in the agostic C–H bond length for complexes **1** and **6** – **11**.

N–C–C^1–C^2 torsion angles which are a measure of the planarity of the ligand, are still small, reflecting the inflexibility of the ligand and actually decrease (8.6° for H, 7.5° for Me and $CHMe_2$, 4.3° for CMe_3; Ph which has other metrics similar to $CHMe_2$ is 6.8°).

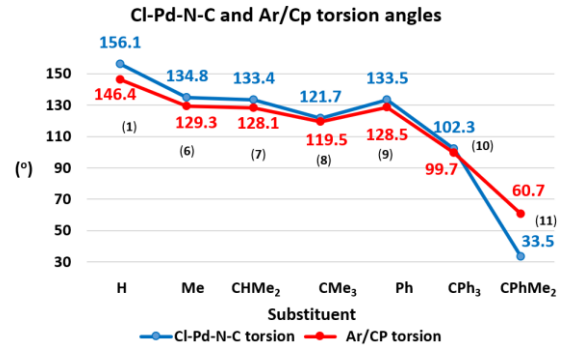

Figure 4. Graphical presentation of the change in the agostic Cl–Pd–N–C and Ar/CP torsion angles for complexes **1** and **6** – **11**.

In this situation, C^2-H deformation does not change much (30.4° for H, 28.2° for Me, 28.1° for $CHMe_2$ and 25.3° for CMe_3, 28.0 for Ph) and the all-important Pd···C^2 separations also do not change significantly from methyl group onwards (2.219 Å for H; 2.195 Å for Me, 2.192 Å for both $CHMe_2$ and CMe_3, 2.196 Å for CMe_3). Graphical presentations of this trend along with those for the Pd···C^1 and Pd···C^3 separations are contained in figures included in table S2 of the ESI.

The lack of disruption of the agostic donation appears to be related to the ability of the ring-A nitrogen to coordinate at different angles to palladium as shown by the Pd–N–C*p* angle (C*p* is the carbon *para*-to the coordinating nitrogen atom) and also the changing Pd–N bond length (figure 5) which essentially means that the Pd–N bond flexes and changes the way this section of the ligand positions. The NBO analysis shows that the agostic C^2–H donation does not change very much as indicated earlier by the C^2–H bond lengths and the syndetic and Pd to C–Hσ* backbonding show a similar result (see table S3 in the ESI). Overall, although there are some indicative changes to the metrics caused by the substituents, there appears to be little steric effect generated to change the donations.

The question then arises as to where significant steric disruption might occur. In assessing the effect of a variety of other substituents it was found that CPh_3 appeared to be a

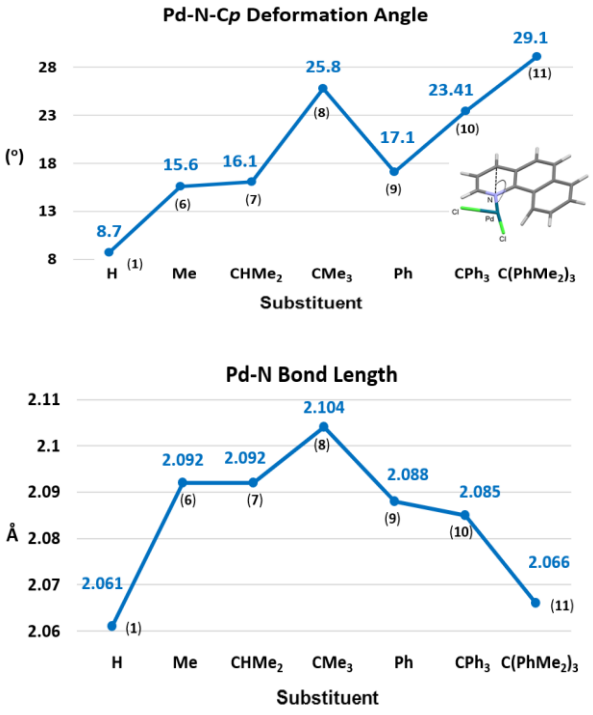

Figure 5. Graphical presentation of the change in the Pd–N–C*p* angle shown in the diagram but represented by the plane-deviation angle on the graph (top) and the Pd–N bond lengths (bottom) for complexes **1** and **8** – **13**.

turning point. In this case, complex **10**, the C^2–H bond shortens to 1.141 Å (1.166 Å for H as substituent) when the Ar/Cp and Cl–Pd–N–C torsion angles change significantly (99.7 and102.3° respectively in **10** compared to 146.4 and 156.1° in **1** where H is the substituent) which essentially means the ligand has rotated about the Pd–N in response to the steric pressure (see figure 6) and pushed the C^2-aromatic ring upwards. With this rotation, the Pd···C^2 separation increases only to 2.225 Å from 2.219 in the more in-plane coordination mode in **1** where the substituent is H.

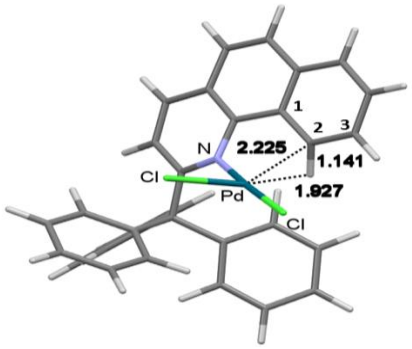

Figure 6. Capped-stick computed structure for complex (**10**). Separation distances shown are in Å.

In addition to this rotation, the Pd–N–C*p* angle change to 154.2º in **10** is smaller than that for the CMe_3 substituent in **8** (164.4º) and the C^2–H bond deformation torsion angle is the smallest yet at 23.7º.The NBO analysis now shows that although the agostic C^2–H σ-bond electron density donation to palladium has come down to 37.3 kcal mol^{-1} in the complex (the range for complexes **1** and **6** to **9** is only 54.9 to 56.4 kcal mol^{-1}) with the steeper angle that the ligand and thus the agostic C^2–H bond C-ring makes with the coordination plane, the syndetic donations do not change much in comparison to complexes **1** and **6** to **9**.

In further steric manipulation, it was found that by adding methyl groups to the 2,6-positions of the phenyl rings of the CPh_3 substituent, the ligand could be forced to rotate sufficiently about the Pd–N bond to form an above-plane orientation consistant with an anagostic interaction (see figure 7). The C^2–H bond length at 1.095 Å is now not significantly different to the other aromatic ring hydrogens and the Pd···H separation at

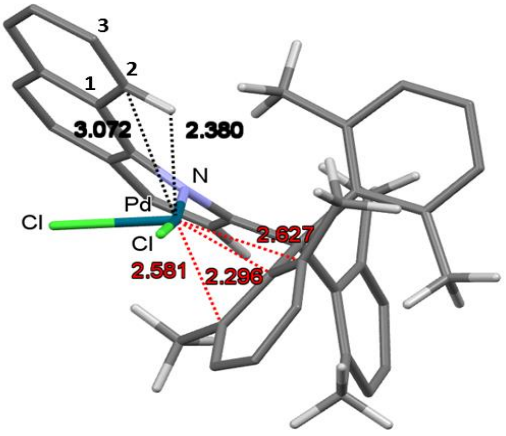

Figure 7. Capped-stick computed structure for complex (**11**). The dashed black line shows the above-plane anagostic interaction and the dashed red line shows the new below-plane interaction. Aromatic ring C–H bond hydrogens apart from that at C^2 have been removed for diagram clarity. Separation distances are in Å.

2.380 Å is similar to those we have found for other anagostic benzo[*h*]quinoline complexes where the positioning of the C^2–H hydrogen is similar.[8] That the complex is clearly under extreme steric pressure is indicated by the Pd–N–C*p* angle which at 150.9º (i.e the deviation is 29.1º) is the largest observed in the present work (for H-substituent complex **1** this angle was 171.3º or otherwise 8.7º and for CPh_3 substituent complex **10**,154.2º or otherwise 25.8º). The NBO analysis shows that there is a small component of C^2–H σ-bond electron density donated to the palladium centre with the *E*(2) value of 4.9 kcal mol^{-1} being in the range of values we have previously suggested may be termed 'preagostic' rather than 'anagostic'.[21] However, there are no syndetic donations observed. It is worth noting here that even though the C^2-aromatic ring is enclined towards the coordination plane at a fairly acute angle (Ar/CP angle 60º) the C^2-carbon is separated from the Pd centre by a distance of 3.072 Å which is apparently too far for π-syndetic donation to develop.

Inspection of the structural features for complex **11** in figure 7 also shows that there are now close approaches made to the Pd centre by carbons of a 2,6-dimethylphenyl ring that lie to the right and below the coordination plane. The shortest of these Pd···C separations is to the *ipso*-carbon at 2.296 Å but there are longer but still relatively close separations involving the two *ortho*-carbons on which the methyl groups reside, at 2.581 and 2.627 Å. The other distinguishing feature is that this phenyl ring is pushed back by nearly 20º where there is no such push-back seen for the aromatic rings of the other 2,6-dimethylphenyl rings of this part of the ligand.

The NBO analysis for the complex shows that the major bonding component involving these close approaches is π-donation from the aromatic ring C*ipso*–C*ortho* bond that lies uppermost towards the palladium centre, to the *trans*-related Pd–Cl* orbital [*E*(2) value, 34.3 kcal mol^{-1}] and the *cis*-related Pd–Cl* orbital [*E*(2) value, 10.2 kcal mol^{-1}] giving what appears to be an η^2-π-bonded aromatic ring.[20] Even though one *ortho*-carbon lies closer to the metal centre (2.581 versus 2.627 Å), there is no π-bonding to the metal from the other aromatic ring C*ipso*–C*ortho* bond and this appears to be related to this bond lying more under the coordination plane than the other interacting C*ipso*–C*ortho* bond which is more in-line with the coordination plane. However, the lower C*ipso*–C*ortho* bond does make a σ-interaction with the metal centre but the *E*(2) value is only 5.4 kcal mol^{-1}, again to the two Pd–Cl antibonding orbitals.

3) Size effect of an *ortho* electron donating substituent

As a departure from adding the substituent only to the position *para*-to the agostic C^2–H bond, we have also placed electron donating substituents in the *ortho*-position in an attempt to not only reinforce the electron donation but also to assess any steric effects for the present benzo[*h*]quinoline complexes that can arise at this position on aromatic rings in general.[18] In our earlier work with the more flexible ligands, S^- substituents placed at these two positions did not give rise to an energy minimised structure[5] but for the present benzo[*h*]quinoline ligand energy minimisation did occur to give complex **12** (figure 8).

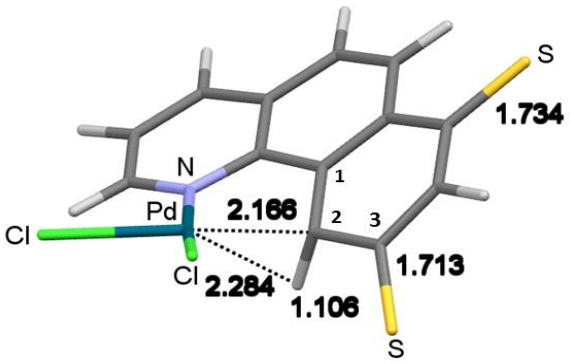

Figure 8. Capped-stick computed structure for complex (**12**). Separation distances are in Å.

At this stage, for convenience when there are 3 substituents, we introduce a system for ease of identification in the text that is the same as shown in the schemes. Thus R^1 on the A-ring is identified by **R^1;** and the *ortho* and *para*-substituents on ring C following by **R^2, R^3** so that complex **12** in figure 8 is represented by **H; S^-, S^-**. The major feature seen in **12** is that the C^2–H bond length at 1.106 Å is now only marginally longer than the other C–H bond lengths in the ligand (range 1.100 to 1.103 Å) indicating little lengthening. However, the Pd···C^2 separation (2.166 Å) is similar to that found for **H; H, S^-** complex **5** (2.162 Å) and whereas the C^2–H bond deformations are similar in both complexes (39.9 and 39.1º for **12** and **5** respectively), the Pd···H separation at 2.284 Å in **12** is now significantly longer than in **5** (1.989 Å).

The reason for these changes can be seen as an apparent steric effect at C^3 in ring C where the S atom is pushed back from the ring plane by 11.4º due to a clash with the adjacent chloro ligand (a space-filled model for these two atoms is shown in figure 9). In addition, the C^2-carbon itself is pushed back out of the plane of the C-ring by 16.3º resulting in severe distortion of the ring and the chloro ligand is pushed upwards out of the coordination plane by 8.9º. There are also significant changes to the other metrics in **12** (see the values in table S2 of the ESI) particularly the Pd···C^1 separation has closed up to 2.284 Å (for complexes **1** to **5** these separations range from 2.921 to 2.939 Å), the Pd···C^3 separation has increased to 3.309 Å (3.239 to 3.290 Å in **1** to **5**) and as a result, the ring has moved down the coordination plane. (see the representations for **12** in figure S2 of the ESI).

The NBO analysis for **H; S^-, S^-** complex **12** shows that the agostic donation is minimal at 4.8 kcal mol^{-1}, there is no π-syndetic component and the Pd to C–H* backdonation is virtually zero. However, as for **H; H, S^-** complex **5** where η^1-Pd–C bonding is present, complex **12** shows the presence of Pd–C bonding components and backbonding into the aromatic ring, particularly from the C^3–S^- (i.e. *ortho*-S^- substituent) bond. Interestingly, the C^1–C^2 and C^2–C^3 bond distances are quite long at 1.465 and 1.477 Å which would suggest significant sp^3 nature when the C–C bonds for the other two aromatic rings range from 1.387 to 1.429 Å and are longer than for the equivalent C–C bonds in complex **5** with only the single S^- substituent in the *para*-position. For S^- substituents at both *ortho* and *para*-positions in **12**, the magnitude of the C^2-atomic charge now decreases to -0.0790 *e* in comparison to *para*-S^- substituted **5** (-0.1077 *e*), the H-atomic charge becomes less positive (0.0335 versus 0.0587 *e*) and the Pd atomic charge also becomes less positive (0.5401 versus 0.5684 *e*).

Given the result for complex **12** where size of the *ortho*-substituent has an effect in terms of clashing with the adjacent chloro ligand, it was of interest to ascertain if electron donation could be generated at both the *ortho* and *para*-positions but with a concommitant closing up of the Pd···C^2 separation. To achieve this, we speculated that hydrogen bonding from an *ortho*-substituent to the adjacent chloro ligand could be beneficial and so placed an NH_2 substituent (*R* value, -0.74; *F* value 0.08[17]) at the ring-C C^3 position. The energy minimised structure for this **H; NH_2, S^-** complex, **13**, is shown in figure 10.

Looking at the metrics for **13**, it is seen that an *ortho*-NH_2 group does achieve a shorter Pd···C^2 separation with the distance now being 2.141 Å which is shorter than that found for **H; H, S^-** complex **5** or **H; S^-, S^-** complex **12** where the separations were 2.162 and 2.166 Å respectively. The closing up in **H; NH_2, S^-**

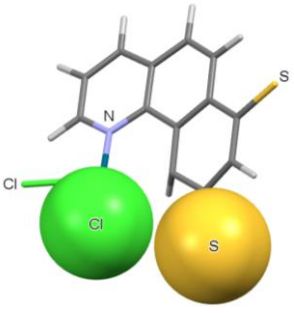

Figure 9. Capped-stick computed structure for complex (**12**) showing space filled Cl and *ortho*-S atoms.

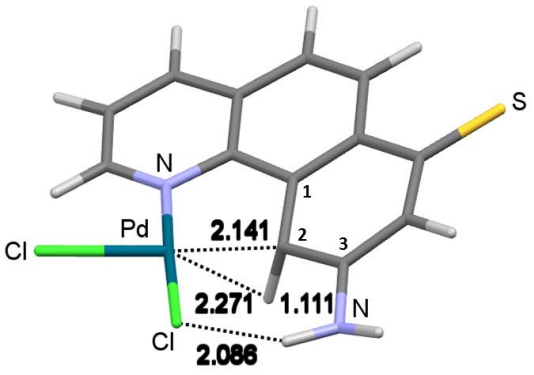

Figure 10. Capped-stick computed structure for complex (**13**) showing space filled Cl and *ortho*-S atoms with separation distances in Å.

complex **13** appears then to be related to development of weak N–H···Cl hydrogen bonding (figures 10 and 11) as was envisaged, where the H···Cl separation is 2.086 Å. This is accompanied by a very large C^2–H bond distortion where the torsion angle is 52°. In comparison to **H; S⁻, S⁻** complex **12**, the C^2–H bond is slightly lengthened in **13** to 1.111 Å (1.106 Å in **12**) and this is reflected in the NBO analysis where the agostic

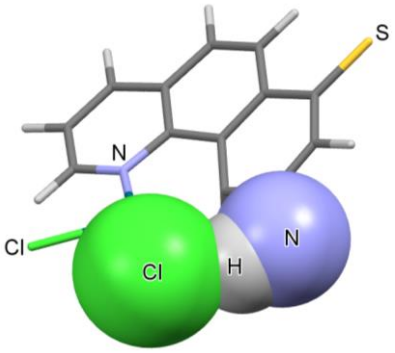

Figure 11. Capped-stick structure of (**13**) showing the space-filled Cl atom and the N and H atoms of the *ortho*-NH_2 substituent.

C^2–H bond donation shows a slight increase [*E*(2) values, 6.4 and 4.8 kcal mol^{-1} for **13** and **12** respectively] and there is again no π-syndetic donation present and as seen for the other complexes. As for complex **12**, there is evidence for Pd–C bond formation in the NBO data for **13** indicating η^1-Pd–C^2 bonding (the Pd···C^3 separation at 3.256 Å is too large to indicate η^2-Pd bonding) and donation components back into the aromatic ring particularly from the *ortho*-nitrogen substituent. In addition, the C^1–C^2 and C^2–C^3 bond distances are longer than the other ring C–C bond distances and similar to those found for complex **12** which again suggests significant sp^3 character. For the atomic charges, the C^2-atomic charge is a little more negative [*q*(C) values, -0.1001 and -0.079 *e* for **13** and **12** respectively], the H-atomic charge is more positive [*q*(H) values, 0.0464 and 0.0335 *e*] and the Pd-atomic charges are not much different [*q*(Pd) values, 0.5441 and 0.5401 *e*].

4) Steric effects at the Carbon *ortho* to nitrogen and electronic manipulation of the agostic interaction.

We have also looked at some exemplars (complexes **14**, **15** and **16** in scheme 3) where the size of the substituent at the carbon lying *ortho* to the coordinating nitrogen atom (A-ring α-carbon) is increased, in an attempt to gauge any effect on the electronic transformation of the agostic interaction into a η^1-Pd–C^2 bond. For this exercise, we have in the first instance compared H and Me groups at the α-carbon and used the strongly π-donating S^- substituent as the electron donor at the position *para* to the agostic carbon which was found to produce the η^1-Pd–C^2 bond transformation.

For perspective, as mentioned in section 1, placing an S^- substituent on complex **1** where the α-carbon is hydrogen to give **H; H, S⁻** complex **5**, results in a shortening of the agostic C–H

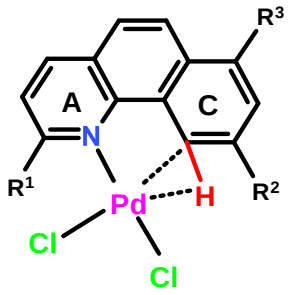

(**14**) R^1 = Me, R^2 = H, R^3 = S^-
(**15**) R^1 = Ph, R^2, R^3 = S^-
(**16**) R^1 = Ph, R^2 = NH_2, R^3 = S^-

Scheme 3. Structures showing the electronic substituents.

bond when the η^1-Pd–C^2 bond is generated as indicated by the shorter Pd–C^2 bond length (2.162 Å in **5**; 2.219 Å in **1**). There was also a larger C–H bond deformation seen (39.1 and 30.4° respectively), a flattening of the Cl–Pd–N–C torsion angle from 156.1 ° in **1** to 164.0° in **5** and the agostic donation *E*(2) energy drops from 55.6 kcal mol^{-1} in **1** to only 11.0 kcal mol^{-1} in **5**.

For further perspective, as mentioned in section 2, the effect of adding a methyl group to the α-carbon of **H; H, H** complex **1** to give **Me; H, H** complex **6** had little effect on the on the agostic donation (the C-H bond length only drops from 1.166 to 1.163 Å and the agostic donation change is neglible) even though there are some quite substantial changes to the way the ligand positions with respect to the coordination plane (the Pd–N–C*p* deformation angle changes from 171.3 to 164.4°; the Cl–Pd–N–C torsion from 156.1 to 134.8° and the Ar/CP torsion angle changes from 146.4 to 129.3° but there is little change to the C–H deformation angle at 30.4 and 28.2°).

Looking now at combining the *para*-S^- ring C substituent of **H; H, S⁻** complex **5** and the α-carbon methyl group ring A substituent of **Me; H, H** complex **6** to give **Me; H, S⁻** complex **14**, it is found that the η^1-Pd–C^2 bond length reduces to 2.153 Å from 2.195 Å in **Me; H, H** complex **6** (this bond length was 2.162 Å in **H; H, S⁻** complex **5**) even though there is not much change in the various torsion angles in the two structures. It is then seen, that the agostic donation for **14** only reduces from 54.9 to 23.7 kcal mol^{-1} whereas when the α-carbon substituent was hydrogen in **H; H, S⁻** complex **5** , the analogous reduction was greater at 55.6 to 11.0 kcal mol^{-1}. This result thus shows that adding a methyl group strengthens the η^1-Pd–C^2 bond (i.e. the observed shorter Pd–C^2 bond length for **14**) and decreases the loss of agostic donation.

In a further examination of a possible interplay of steric and electronic effects, it was decided to change the size of the α-carbon substituent of the ligand A-ring just as was done for **Me; H, S⁻** complex **14** above, but to now include *ortho*-S^- or NH_2 substituents as was done in complexes **12** and **13** in section 3. However, instead of using an α-carbon Me group as above, a

phenyl substituent was used this time (section 2 showed that Ph and Me groups produced similar steric effects) giving **Ph; S⁻, S⁻** complex **15** and **Ph; NH₂, S⁻** complex **16**.

For the exercise of comparing the structures of **15** and **16** with those of **H; S⁻, S⁻** complex **12** and **H; NH₂, S⁻** complex **13** we have again employed graphical representations and have also included the parent complexes **1** and **9** where the α-carbon substituent on ring A is either H or Ph, so that multi-component comparisons can be carried out. Figure 12 then shows how the Pd···C² separation is significantly shorter for **Ph; H, H** complex **9** than for **H; H, H** complex **1** and then both become much shorter in the **S⁻,S⁻** η¹-Pd complexes where the *ortho*-S⁻ group exerts a

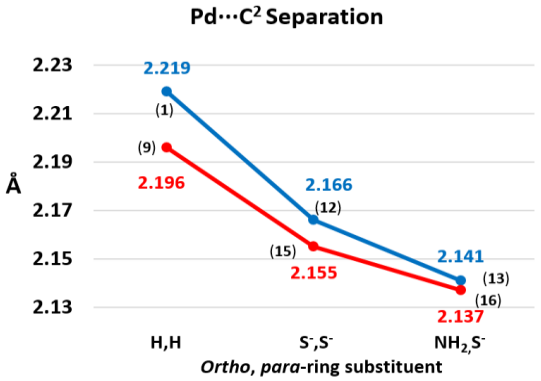

Figure 12. Graphical representation of the change in Pd···C² separations. Blue data, A-ring α-carbon substituent H. Red data, A-ring α-carbon substituent Ph. Complex number in parentheses.

steric effect (**12** and **15**) and then decreases again when the *ortho*-NH_2 group pulls the aromatic ring inwards with N–H···Cl hydrogen bonding.

Turning to how the ligand positions itself as the Pd···C² separations get smaller, it is seen in figure 13 that the Cl–Pd–N–C torsion angle which represents the rotation around the N–Pd bond and essentially how the ligand postions above the coordination plane, the angle is much smaller in agostic phenyl complex **9** than agostic H complex **1** indicating the ligand rotates upwards. The angles then do not increase much in the η¹-Pd **S⁻, S⁻** complexes **12** and **15** but then increase more with the **NH₂, S⁻** complexes **13** and **16** with the slight flattening of the angle indicating the ligand rotates downwards a little.

The Pd–N–C*p* deformation angles (figure 13; again, the actual measured angle which represents the way the ligand is pushed upwards at this point) decrease in going from agostic complex **1** to **9** and then both decrease significantly in the η¹-Pd **S⁻,S⁻** complexes **12** and **15** as the Pd···C² separations decrease (figure 12) and then increase in the η¹-Pd **NH₂, S⁻** complexes **13** and **16** as the hydrogen bonding pulls the other end of the ligand (i.e the C-ring) back inwards. At the same time as these features occur, the Pd–N bond length (figure 13) increases on going from **H; H, H** complex **1** to **Ph; H, H** complex **9**. Then, on proceding to the **S⁻,S⁻** substituents, for the A-ring Ph complex **15** the bond length increases whereas for the A-ring H complex **12** there is a decrease. With the change to **NH₂** and **S⁻**, the Pd–N bond lengths then become smaller. Over the 3 different features then

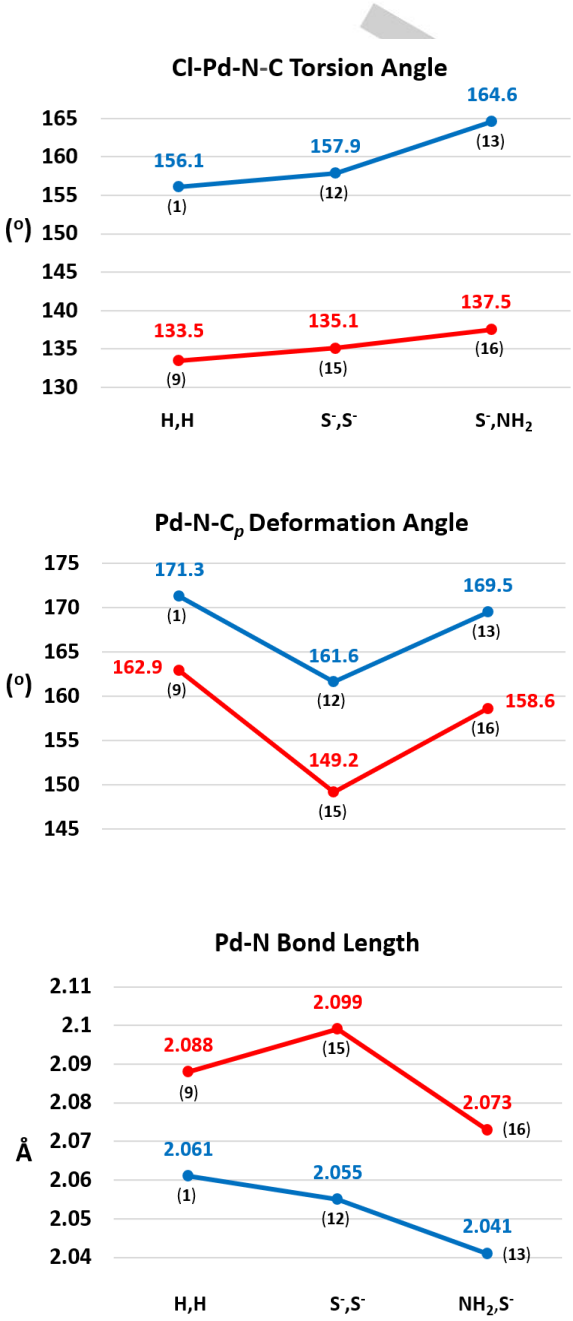

Figure 13. Graphical representation of the change in Cl–Pd–N–C and the measured Pd–N–C*p* torsion angles and the Pd–N bond length. Blue data, A-ring α-carbon substituent H. Red data, A-ring α-carbon substituent Ph. Complex number in in parentheses .

there is a subtle rearrangement that accommodates coordination of the ligand.

The final features being examined here are the C–H bond length and deformation from the aromatic ring plane. Figure 14 shows that both of these do not vary much when the A-ring α-carbon substituents are H or Ph in the agostic complexes **1** and

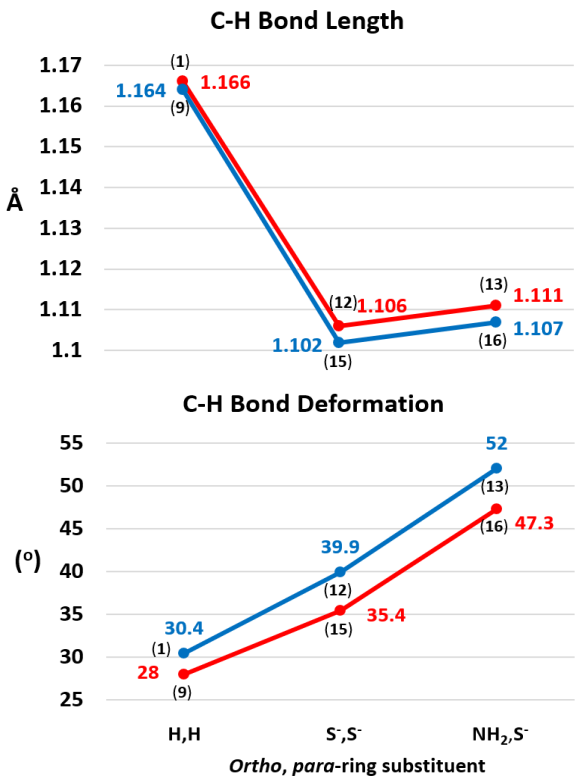

Figure 14. Graphical representation of the change in Pd–N–C–C[1] and Pd–N–Cp torsion angles and the Pd–N bond length. Blue data, A-ring α-carbon substituent H. Red data, A-ring α-carbon substituent Ph. Complex number in in parentheses.

9 but when these complexes shift to being η^1 with the C-ring **S⁻, S⁻** substituents the bond lengths which are an indication of the amount of agostic donation, decrease to the point of a switch-off of this interaction. Pulling the ligand back in with the NH_2 substituent increases this donation only marginally. At the same time, the C–H bond deformations increase when the η^1-Pd–C bonds are formed in **12** and **15**, reaching the higest value of all at 52° in **H; NH₂, S⁻** complex **13** containing the *ortho*-NH_2 and is not much lower when the A-ring α-carbon substituent is Ph (47.3°) in **16**. The Pd–C[2]–H angles of the complexes with the *ortho*-S or NH_2 substituents range from 82.0° to 87.2° (not shown in the figures) and are typical of η^1-Pd–C complexes in general[20] The complexes also exhibit C-ring C^1–C^2 and C^2–C^3 bond lengths that suggest significant sp^3 character. This is also apparent for the bonds attached to the C-ring *para*-carbon atom whereas the remaining C-ring bonds are more typical of the other aromatic rings. The NBO analysis again shows delocalisation of the π-electron density away from the *para*-S atom through the ring to C^2 and on into the orbitals involving the η^1-Pd–C bonding components indicating that the C-ring is showing significantly reduced aromaticity.

The movement of electron density towards the Pd centre would then suggest that positive charge on the metal should become less positive when there are 2 S⁻ substituents present and this is seen where *q*(Pd) for **H; S⁻, S⁻** complex **12** is lower at 0.5041 *e* and higher at 0.5684 *e* in **H; H, S⁻** complex **5**. Figure 15 below shows a summary of how the Pd atomic charges perform for the various electron donating substituents (to the right of the dashed red line) and also includes the trend for the electron withdrawing substituents (left of the dashed red line). Keeping in mind again that the various electronic substituents do not have the same electron donating or withdrawal abilities in terms of *F* or *R* values, the donation data still shows a decreasing trend in the positive *q*(Pd) values. It is worth noting here that with the addition of the η^1-Pd–C bonding system to $PdCl_2$, 'Pd^{3+}' could be invoked but the reducing positive charge clearly points away from this so that a delocalised Pd^{2+} anion of the form [$PdCl_2$(σ-bond carbon)]⁻ may be present.

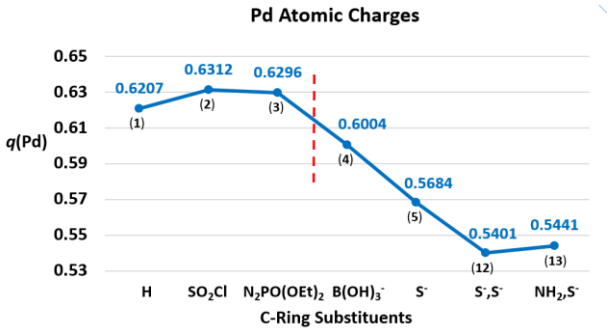

Figure 15. Graphical presentation of the change in Pd atomic charges [*q*(Pd)] for complexes **1** – **5**, **12** and **13**. The dashed red line shows the change-over from electron withdrawal to electron donation.

Conclusion

In summary, we have looked at how agostic interactions and the associated π-syndetic donations perform under the conditions of electronic and steric influences in the relatively inflexible benzo[*h*]quinoline ligand and then examined how η^1-Pd–C bond formation can be induced and then influenced. For the first of these manipulations, it is found that the σ or π-electron withdrawing substituents used at the *para*-position of the ligand C-ring do not effect the agostic or π-syndetic donations to any extent, whereas the σ or π-electron withdonating substituents cause a dramatic change to η^1-Pd–C bond formation where there is still some agostic donation present but no longer any π-syndetic donation.

Examination of the influence of steric effects generated at the α-carbon of ring A, it is seen that moving through the series H, Me, Ph, $CHMe_2$, CMe_3 causes the ligand to rotate up over the coordination plane somewhat but the agostic donations do not change that much whereas with the ligand rotation upwards, the angle the ligand C-ring faces the metal coordination plane decreases significantly (146.4 to119.5° for the series) but the π-syndetic donations do not increase by much [*E*(2) values range from 12.8 to 15.0 kcal mol^{-1} for the series]. A CPh_3 substituent appears to be a turning point for steric influence with the agostic donation droping significantly but not the π-syndetic donation

and C(Ph-2,6-Me_2)$_3$ turns the donations off giving an anagostic complex.

Introducing an *ortho*-S^- substituent to the C-ring which already contains a *para*-S^- substituent, pushes the ring away from the metal centre by a steric clash with the adjacent chloro ligand and hardly influences the η^1-Pd–C bond distance but the reduced agostic donation found when only the *para*-S^- substituent is present, becomes mostly absent. Replacing the *ortho*-S^- substituent with the π-donating NH_2 substituent, draws the C-ring back in by weak N–H hydrogen bonding with the adjacent chloro ligand and this shortens the η^1-Pd–C bond distance significantly but the very small agostic donation found when the substituent was S^- hardly changes.

Throughout the changes to the various substituents of all the complexes reported, it is clear that in the absence of much ligand flexibility, the benzo[*h*]quinoline ligand is under some stress to coordinate at all. However, with various changes to such features as the Pd–C bond distance, distortions in the manner the N coordinates to palladium (i.e. the Pd–N–C*p* angle), rotation about the Pd–N bond and the severe distortion of the C^2–H bond out of the C-ring plane, favourable coulombic interactions and even the formation of η^1-Pd–C bonding, it is clear that the ligand is able to adjust to the various pressures. The coordination of the nitrogen atom to Pd is the major influencing factor however.

Overall, this work shows that agostic and π-syndetic donations can still be present for a ligand such as benzo[*h*]quinoline but electronic influences can easily convert the system to η^1-Pd–C bonding. These results are important as in terms of the CMD/AMLA mechanism for Pd-C bond formation, it shows that substituent effects can play a significant role. With the ever increasing sophistication of ligand directed aromatic ring C-H bond activations being seen at present, electronic and steric effects could well determine whether C-H bond activation occurs at all.

Experimental Section

Computational details. Density functional theory (DFT) based geometry optimizations and vibrational calculations for the complexes were performed using the dispersion corrected PBE-D3[9] functional within the Gaussian09 (G09)[22] software. A triple-zeta high quality basis set (aug-cc-pVTZ-PP)[23] was employed for Pd together with a scalar relativistic energy consistent Stuttgart pseudopotentials for Pd; cc-pVTZ[24] for the attached ancillary ligands (Cl atoms), agostic hydrogen and nitrogen (attached to the metals) and double-zeta quality basis set (cc-pVDZ)[24] was used for the remainder of atoms. No imaginary frequencies were found in the vibrational analysis. The NBO calculations were performed with the NBO6.0 package.[25] Comparisons of the present second order perturbation energies [*E*(2) values] with those published elsewhere are made within the same basis set and functional and in relation to other work[6,15] are not expected to involve significant basis set superposition error (BSSE).[14] For the QTAIM analyses, the input files (.wfx) were obtained from G09[22] and the QTAIM calculations were performed with the AIMALL software.[26]

.

Supporting Information (see footnote on the first page of this article). For complexes **1** to **16**: Structures showing the A and C-ring substituents; Mercury diagrams; Capped-stick structural diagrams showing the close approach of the aromatic ring in relation to the metal coordination plane; Cartesian coordinates; Selected Structural data; NBO Analysis *E*(2) data; Selected Atomic Charge (*q*) data; Full data table, second order perturbation energy *E*(2) values (kcal mol^{-1}) for donor-acceptor NBO interactions.

Keywords: C−H bond activation • agostic interactions • syndetic donation • η^1-Pd–C bonding • cyclometallation reactions

[1] See for example: a) M. Pfeffer, *Pure Appl. Chem*. **1992**, *64*, 335–342; b) I. Omae, *Coord. Chem. Rev*. **2004**, *248*, 995–1023; c) A. D. Ryabov, *Synthesis* **1985**, 233–252; d) J. Dupont, M. Pfeffer, J. Spencer, *Eur. J. Inorg. Chem*. **2001**, 1917–1927; e) R. B. Bedford, *Chem. Commun*. **2003**, 1787–1796; f) J. Dupont, C. S. Consorti, J. Spencer, *Chem. Rev*. **2005**, *105*, 2527–2571; g) J. P. Djukic, J. B. Sortais, L. Barloy, M. Pfeffer, *Eur. J. Inorg. Chem*. **2009**, 817–853; h) M. Albrecht, *Chem. Rev*. **2010**, *110*, 576–623; i) L. Cuesta, E. P. Urriolabeitia, *Comments Inorg. Chem.* **2012**, *33*, 55–85.

[2] a) E. M. *Beck,* M. J. Gaunt*,* in *Topics* in *Current Chemistry*: *C–H Activation*, Vol. 292 (Eds: J. Q. Yu, Z. J. Shi*),* Springer-Verlag*:* Berlin*,* **2010***, pp* 85–121; b) J. Yamaguchi, A. D. Yamaguchi, K. Itami, *Angew. Chem. Int. Ed.* **2012**, *51*, 8960−9009; c) J. Wencel-Delord, T. Dröge, F. Liu, F. Glorius, *Chem. Soc. Rev.* **2011**, *40*, 4740–4761; d) T. W. Lyons, M. S. Sanford, *Chem. Rev.* **2010**, *110*, 1147–1169; e) O. Baudoin, *Chem. Soc. Rev.* **2011**, *40*, 4902–4911; f) K. M. Engle, T.-S. Mei, M. Wasa, J.-U. Qu, *Acc. Chem. Res*. **2012**, *45*, 788–802; h) A. F. M. Noisier, M. A. Brimble, *Chem. Rev*. **2014**, *114*, 8775–8806; i) G. Rouquet, N. Chatani, *Angew. Chem. Int. Ed.* **2013**, *52*, 11726−11743 and refs cited therein; j) I. P. Beletskaya, A. V. Cheprakov, *J. Organomet. Chem.* **2004**, *689*, 4055−4082. k) F. Zhang, D. R. Spring, *Chem. Soc. Rev*. **2014**, *43*, 6906–6919. l) S. St John-Campbell, J. A. Bull, *Org. Bimol. Chem*. **2018**, *16*, 4582–4595. m) Y.-F. Yang, X. Hong, J.-Q. Yu, K. N. Houk, *Acc. Chem. Res*. **2017**, *50*, 2853–2860.

[3] a) M. Lein, *Coord. Chem. Rev*. **2009**, *253*, 625–634; b) M. Brookhart, M. L. H. Green, G. Parkin, *Proc. Natl. Acad. Sci. U. S. A.* **2007**, *104*, 6908–6914; c) W. Scherer, G. S. McGrady, *Angew. Chem. Int. Ed.* **2004**, *43*, 1782–1806; d) J. J. Schneider, *Angew. Chem., Int. Ed.* **1996**, *35*, 1068–1076; e) R. H. Crabtree, *Angew. Chem., Int. Ed. Engl.* **1993**, *32*, 789–805; f) M. Brookhart, M. L. H. Green, *J. Organomet. Chem.* **1983**, *250*, 395–408.

[4] a) D. L. Davies, S. M. A. Donald, S. A. Macgregor, *J. Am. Chem. Soc*. **2005**, *127*, 13754−13755. b) D. L. Davies, S. A. Macgregor, C. L. McMullin, *Chem. Rev.* **2017**, *117*, 8649–8709. c) B. P. Carrow, J. Sampson, L. Wang, *Isr. J. Chem.* **2019**, *59,* 1–30.

[5] a) M. A. Sajjad, K. E. Christensen, N. H. Rees, P. Schwerdtfeger, J. A. Harrison, A. J. Nielson, *Chem. Commun*. **2017**, *53*, 4187–4190; b) M. A. Sajjad, K. E. Christensen, N. H. Rees, P. Schwerdtfeger, J. A. Harrison, A. J. Nielson, *Dalton Transactions* **2017**, *46*, 16126-16138; c) M. A. Sajjad, J. A. Harrison, A. J. Nielson, P. Schwerdtfeger, *Organometallics* **2017**, *36,* 4231–4237; d) M. A. Sajjad, J. A. Harrison, A. J. Nielson, P. Schwerdtfeger, *Organometallics* **2018**, *37*, 3659–3669. (e) J. A. Harrison, A. J. Nielson, M. A. Sajjad, P. Schwerdtfeger, *Organometallics* **2019**, *38*, 1903–1916.

[6] Y. Cornaton, J.-P. Djukic, *Phys.Chem.Chem.Phys*. **2019**, *21*, 20486–20498.

[7] a) B. N. Cockburn, D. V. Howe, T. Keating, B. F. G. Johnson, J. Lewis, *J. C. S. Dalton*, **1973**, 404–410; b) R. Bhawmick, H. Biswas, P. Bandyopadhyay, *J. Organometallic. Chem*. **1995**, *498*, 81–83. c) A. R. Dick, J. W. Kampf, M. S. Sanford, *Organometallics* **2005**, *24*, 482–485. d) A. R. Dick, M. S. Remy, J. W. Kampf, M. S. Sanford, *Organometallics* **2007**, *26*, 1365–1370. e) A. J. Deeming, I. P. Rothwell, M. B. Hursthouse, L. New, *J. Chem. Soc. Dalton*, **1978**, 1490–1496.

[8] J. A. Harrison, A. J. Nielson, M. A. Sajjad, P. Schwerdtfeger, *Eur. J. Inorg. Chem*. **2017**, 2255–2264.

[9] a) J. P. Pedrew, K. Burke, M. Ernzerhof, *Phys. Rev. Lett*. **1996**, *77*, 3865–3868; b) S. Grimme, J. Antony, S. Ehrlich, H. Krieg, *J. Chem. Phys.* **2010**, *132*, 154104−154119.

[10] Q. Lu, G. Bistoni, *Angew. Chem., Int. Ed*. **2018**, *57*, 4760–4764.

[11] a) D. A. Pantazis, J. E. McGrady, F. Maseras, M. Etienne, *J. Chem. Theory Comput.* **2007**, *3,* 1329–1336; (b) C. Lepetit, J. Poater, M. E. Alikhani, B. Silvi, Y. Canac, J. Contreras-Garcia, M. Sola, R. Chauvin, *Inorg. Chem.* **2015**, *54*, 2960–2969.

[12] For more recent X-ray crystal structures showing the distorted aromatic ring C–H bond, see a) R. Beck, S. Camadamli, H.-F. Klein, *Eur. J. Inorg. Chem*. **2018**, 608–611; b) L. S. Jongbloed, D. García-López, R. van Heck, M. A. Siegler, J. J. Carbó, J. I. van der Vlugt, *Inorg. Chem*. **2016**, *55*, 8041−8047; c) L. S. Jongbloed, B. de Bruin, J. N. H. Reek, M. Lutz, J. I. van der Vlugt, *Chem. Eur. J.* **2015**, *21*, 7297–7305; d) M. S. L. Latos-Grazynski, L. Szterenberg, J. Panek, Z. Latajka, *J. Am. Chem. Soc.* **2004**, *126*, 4566–4580. For pincer ligand complexes, see the references in S. Murugesan, B. Stoeger, E. Pittenauer, G. Allmaier, L. F. Veiros, K Kirchner, *Angew. Chem., Int. Ed.* **2016**, *55*, 3045–3048.

[13] a) F. Weinhold, C. Landis, *Valency and bonding: A Natural Bond Orbital Donor-Acceptor Perspective;* Cambridge University Press:

Cambridge, England, **2005**; b) F. Weinhold, C. Landis, E. D. Glendenning, *Int. Rev. Phys. Chem.* **2016**, *35*, 399–440.
[14] a) A. J. Stone, *J. Phys. Chem. A* **2017**, *121*, 1531−1534; b) F. Weinhold, E. D. Glendening, J. *Phys. Chem. A* **2018**, *122*, 724−732; c) A. J. Stone, KSzalewicz, *J. Phys. Chem. A* **2018**, *122*, 733−736.
[15] D. H. Binh, M. Milovanovic, J. Puertes-Mico, M. Hamdaoui, S. D. Zaric and J.-P. Djukic, *Chem. Eur. J.* **2017**, *23*, 17058–17069.
[16] T. S. Thakur, G. R. Desiraju, *TheoChem*, **2007**, *810*, 143–145.
[17] C. Hansch, A. Leo, R. W. Taft, *Chem. Rev.* **1991**, *97*, 165-195.
[18] M. B. Smith in March's *Advanced Organic Chemistry: Reactions, Mechanism and Structure*, 7th Ed, Wiley, **2013**.
[19] a) R. F. W. Bader in *Atoms in Molecules: A Quantum Theory*, The Clarendon Press, Oxford, **1990**; b) R. F. W. Bader, *Chem. Rev*. **1991**, *91*, 893–928; c) P. Popelier in *Atoms in Molecules: An Introduction*, Prentice Hall, Pearson Education Ltd, **2000**.
[20] S. M. Hubig, S. V. Lindeman, J. K. Kochi, *Coord. Chem. Rev*. **2000**, *200–202*, 831–873.
[21] J. A. Harrison, A. J. Nielson, M. A. Sajjad, P. Schwerdtfeger, *Eur. J. Inorg. Chem*. **2017**, 5485–5496.
[22] M. J. Frisch, G. W. Trucks, H. B. Schlegel, G. E. Scuseria, M. A. Robb, J. R. Cheeseman, G. Scalmani, V. Barone, B. Mennucci, G. A. Petersson, H. Nakatsuji, M. Caricato, X. Li, H. P. Hratchian, A. F. Izmaylov, J. Bloino, G. Zheng, J. L. Sonnenberg, M. Hada, M. Ehara, K. Toyota, R. Fukuda, J. Hasegawa, M. Ishida, T. Nakajima, Y. Honda, O. Kitao, H. Nakai, T. Vreven, J. A. Jr. Montgomery, J. E. Peralta, F. Ogliaro, M. Bearpark, J. J. Heyd, E. Brothers, K. N. Kudin, V. N. Staroverov, R. Kobayashi, J. Normand, K. Raghavachari, A. Rendell, J. C. Burant, S. S. Iyengar, K. Tomasi, M. Cossi, N. Rega, J. M. Millam, M. Klene, J. E. Knox, J. B. Cross, V. Bakken, C. Adamo, J. Jaramillo, R. Gomperts, R. E. Stratmann, O. Yazyev, A. J. Austin, R. Cammi, C. Pomelli, J. W. Ochterski, R. L. Martin, K. Morokuma, V. G. Zakrzewski, G. A. Voth, P. Salvador, J. J. Dannenberg, S. Dapprich, A. D. Daniels, O. Farkas, J. B. Foresman, J. V. Ortiz, J. Cioslowski, D. J. Fox, *Gaussian 09*, Revision D.01; Gaussian, Inc.; Wallingford, CT, 2009.
[23] K. A. Peterson, D. Figgen, M. Dolg, H. Stoll, *J. Chem. Phys.* **2007**, *126*, 124101–124112.
[24] T. H. Jr. Dunning, *J. Chem. Phys.* **1989**, *90*, 1007−1023.
[25] E. D. Glendening, J. K. Badenhoop, A. E. Reed, J. E. Carpenter, J. A. Bohmann, C. M. Morales, C. R. Landis, F. Weinhold, *NBO*, version 6.0, Theoretical Chemistry Institute, University of Wisconsin: Madison, WI, **2013**. See the following: http://nbo6.chem.wisc.edu/.
[26] AIMAll (version 16.08.17), T. A. Keith, TK Gristmill Software, Overland Park KS, USA, **2016**, http://aim.tkgristmill.com.

FULL PAPER

DFT calculations show that agostic complexes of the form $[PdCl_2(L)]$ (L = benzo[*h*]quinoline and substituted benzo[h]quinolines) can be converted to η^1-complexes by electron-donating substituents. Various combinations of steric and electronic effects are able to influence agostic and syndetic donations and the magnitude of the η^1-Pd–C bonding system.

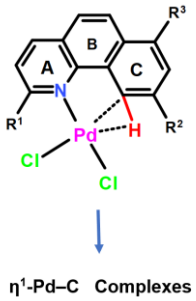

* η^1-Pd–C complexes